Contract No:

This document was prepared in conjunction with work accomplished under Contract No. DE-AC09-08SR22470 with the U.S. Department of Energy (DOE) Office of Environmental Management (EM).

Disclaimer:

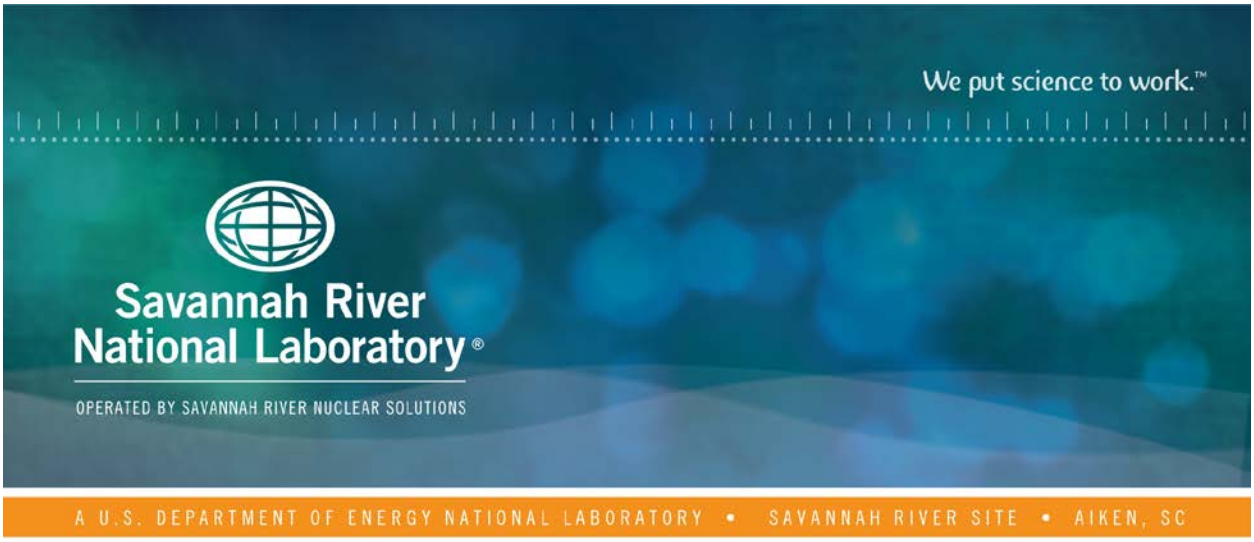

Final Report for PDRD SR16009

Durable Water Splitting using Thermochemical Cycles of Nanostructured Metal Oxides

George Larsen

Simona Murph

Lucas Angelette

Kaitlin Lawrence

September 2018

SRNL-TR-2018-00265

DISCLAIMER

Printed in the United States of America

Prepared for
U.S. Department of Energy

SRNL-TR-2018-00265
Revision 0

Keywords: *Tritium, Glovebox, Water Processing*

Retention: *Permanent*

Final Report for PDRD SR16009
Durable Water Splitting using Thermochemical Cycles of Nanostructured Metal Oxides

G. K. Larsen
S. E. H. Murph
L. M. Angelette
K. J. Lawrence

September 2018

Prepared for the U.S. Department of Energy under contract number DE-AC09-08SR22470.

Savannah River National Laboratory™
OPERATED BY SAVANNAH RIVER NUCLEAR SOLUTIONS

AUTHORS:

G. K. Larsen, Tritium Process Science Group Date

S. E. H. Murph, Tritium Process Science Group Date

L. M. Angelette, Hydrogen Processing Group Date

K. J. Lawrence, Tritium Process Science Group Date

TECHNICAL REVIEW:

P. Beaumont, Hydrogen Processing Group Date

APPROVAL:

R. W. Allgood, Manager Date
Tritium Process Science Group / Hydrogen Processing Group

EXECUTIVE SUMMARY

The Tritium Facility process for stripping tritium from the glovebox atmosphere currently relies on the use of hot magnesium beds (mag beds) to "crack" tritiated water, releasing hydrogen isotopes as a gas. This is a safe and effective process for recovering hydrogen isotopes from water for further processing. However, due to the thermodynamic properties of magnesium, mag beds are single use - once the magnesium metal is converted to magnesium oxide the bed must be replaced. Replacing mag beds is a labor-intensive and operationally complex task. In order to streamline operations and reduce costs, it is desirable to develop a reusable system that recovers hydrogen isotopes from water, while safely sequestering oxygen in a stable form.

The following document reviews the results from the Plant Directed Research, Development, and Demonstration (PDRD) project "Durable Water Splitting using Thermochemical Cycles of Nanostructured Metal Oxides" (SR16009), which had the specific goal of developing a process for stripping tritium from the glovebox atmosphere that eliminates magnesium beds. The research focused on using the reduction-oxidation cycles of metals to create a reusable system that behaved similarly to the current process. The concept is straightforward; a tritium-contaminated steam passes over a hot metal bed, converting the metal to a metal oxide and liberating hydrogen. The bed is regenerated by converting the metal oxide back to a bare metal using protium gas, creating a clean water stream. Free oxygen is not produced during the cyclical process, making it safe for use in a hydrogen processing facility. The only by-product is detritiated water, which could simplify disposal over the current mag bed process. An experimental down-selection of materials was conducted, and porous zero valent iron (p-ZVI) was identified as an ideal candidate base material due to its low cost, large hydrogen generation capacity, and moderate operational temperatures. Further investigations of p-ZVI were conducted to better understand how a bed composed of such material would behave in the facility. In particular, the thermal and physical properties were assessed, along with long term cycling and isotope effects. The results indicate that p-ZVI beds could serve as low cost, reusable replacements for mag beds in the Tritium Facility.

TABLE OF CONTENTS

LIST OF TABLES

LIST OF FIGURES

LIST OF ABBREVIATIONS

AMSBs	ambient molecular sieve beds
DF	decontamination factor
DTA	differential thermal analysis
k	Thermal conductivity
PDRD	Plant Directed Research, Development, and Demonstration
ppm	parts-per-million
p-ZVI	porous zero valent iron
RGA	residual gas analyzer
SEM	scanning electron microscopy
SRNL	Savannah River National Laboratory
ZBR	Z-Bed Recovery

1.0 Introduction

All process equipment in the Tritium Facility are located within nitrogen gloveboxes, which provide containment for any tritium that escapes during processing. In order to minimize emissions, all tritium that reaches these gloveboxes must be also captured and recovered. This is done by continually recirculating the glovebox atmosphere through tritium stripper systems. The stripper systems work by combusting tritium with ambient oxygen to form water, which is subsequently collected on ambient molecular sieve beds (AMSBs). It is important to note that water accumulation on the AMSBs includes tritiated water formed in the stripper system (internal) and any water that enters the glovebox from process rooms (external). External water ingress arises from glovebox openings (e.g., access during maintenance) and due to diffusion since the gloveboxes are held at slightly negative pressure relative to the process rooms. Current facility operations are such that the majority of water originates external to the gloveboxes. Therefore, AMSBs trap and store large volumes of water with relatively low levels of tritium.

When the AMSBs reach their water loading capacity, they are regenerated by heating the bed to a high temperature to drive off the absorbed water. The water vapor that evolves during AMSB regeneration is processed by the Z-Bed Recovery (ZBR) system to recover any tritium. The ZBR system is essentially a water "cracking" process. Water vapor from the AMSBs, along with a carrier gas (typically protium), are passed through a bed of hot magnesium metal mixed with stainless steel springs (mag beds), to oxidize magnesium and release the hydrogen isotopes for tritium recovery. Due to the thermodynamic properties of magnesium, mag beds are single use - once the magnesium metal is converted to magnesium oxide the bed must be replaced. The spent mag beds, along with the trapped oxygen, exit the process as tritiated metal-oxide waste which is then disposed of on-site as low-level waste.

The cost of the mag bed cartridges varies but range from $35,000 to $61,000 each. About 13 mag bed cartridges are consumed per year representing a material cost of approximately $500,000 per year, according to 2013 data [1]. Not only does the ZBR system process generate magnesium-oxide waste, the replacement and maintenance processes are labor intensive and require an additional isotopic gas separation load of over 130,000 STP-L per year of low tritium content (<0.5% T). In order to streamline operations and reduce costs, it is desirable to develop replacements for mag beds that are reusable and recover hydrogen isotopes from water, while safely sequestering oxygen in a stable form.

The following document reviews the results from the Plant Directed Research, Development, and Demonstration (PDRD) project "Durable Water Splitting using Thermochemical Cycles of Nanostructured Metal Oxides" (SR16009), which has the specific goal of developing a process for stripping the glovebox atmosphere that eliminates magnesium beds. The research focused on using the reduction-oxidation cycles of metal/metal oxides to create a reusable system that is easily integrated into the current process. The concept is straightforward. Similar to the mag bed process, it works by passing the tritium-contaminated steam over a hot metal bed, converting the metal to a metal oxide and liberating hydrogen. However, when the chemical reaction is complete the metal oxide can be reduced back to a bare metal using protium gas, creating a clean water stream (**Figure 1-1**). Free oxygen is not produced during the cyclical process, making it safe for use in a hydrogen processing facility. The only by-product is detritiated water, which could simplify disposal over the current mag bed process. An experimental down-selection of materials was conducted, and porous zero valent iron (p-ZVI) was identified as an ideal candidate base material due to its low cost, large hydrogen generation capacity, and moderate operational temperatures. Further investigations of p-ZVI were conducted to better understand how a bed composed of such material

would behave in the facility. In particular, the thermal and physical properties were assessed, along with long term cycling and isotope effects. The results indicate that p-ZVI beds could serve as low cost, reusable replacements for mag beds in the Tritium Facility.

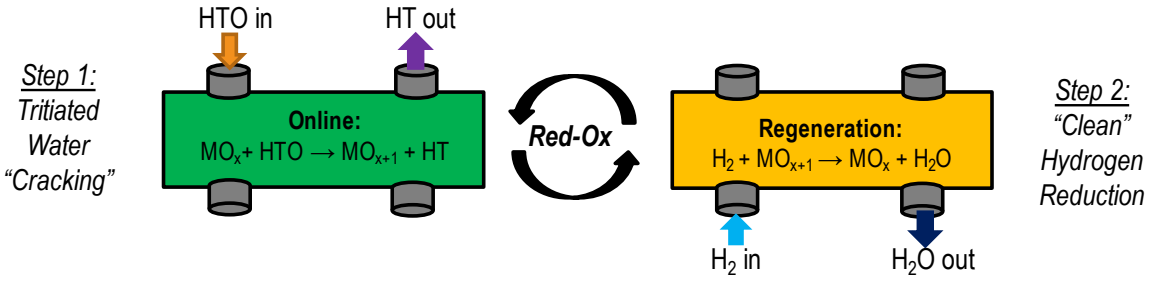

Figure 1-1. Schematic of the reversible metal oxidation process for water splitting. In Step 1 tritiated water oxidizes a metal, creating a metal oxide and liberating hydrogen. In Step 2 protium is used to reduce the metal oxide back to a metal, creating "clean" water.

2.0 Material Down-Selection

2.1 Nanostructured Metal Oxides

The project was motivated by reports in the literature of low temperature thermochemical water splitting enabled by nanostructured metal oxides. In particular, it was found that nanostructured chromium doped cerium oxide (Cr-CeO_2: $Ce_{0.67}Cr_{0.33}O_{2.11}$) could repeatably generate hydrogen in a closed thermochemical cycle, where the maximum temperature was 465 °C [2]. Therefore, the initial research focused on nanostructured ceria for reversible water splitting.

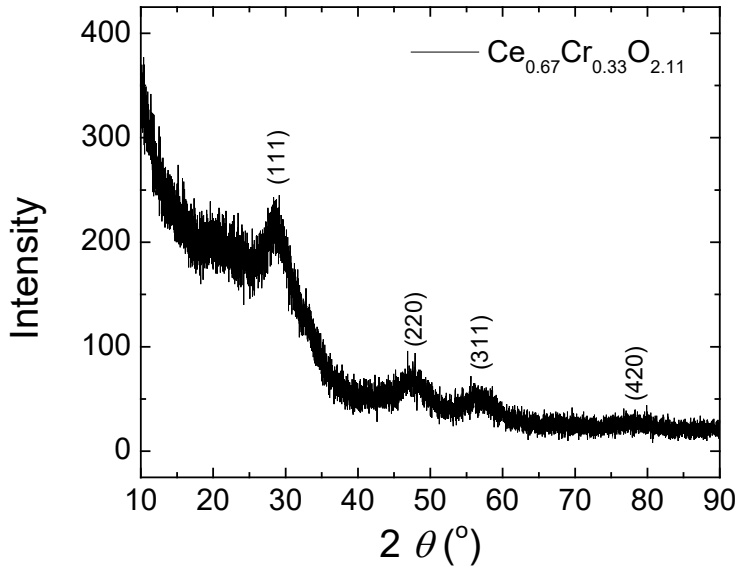

Figure 2-1. X-ray diffraction data of Cr-CeO_2 synthesized via a hydrothermal method, with peak attributions from Ref. [2].

Different ceria-based nanoparticles were acquired to test for their water splitting properties. Since chromium-doped ceria had exhibited positive results in the literature, Cr-CeO_2 (33% doped) was obtained from The University of Georgia, which synthesized the material using hydrothermal techniques following the procedures outlined in Ref 2. X-ray diffraction peaks match those of the fluorite structure observed in Ref. 2 (**Figure 2-1**). Cr-CeO_2 was also obtained by in-house synthesis using a co-precipitation method. Additional ceria nanoparticles were also obtained from a commercial supplier, Cerion: CeO_2, Zr-CeO_2 (18% doped), and Fe_2O_3-CeO_2 (50% doped). Due to their small sizes, the nanoparticles were dried onto kieselguhr for support during experimental measurements (**Figure 2-2**).

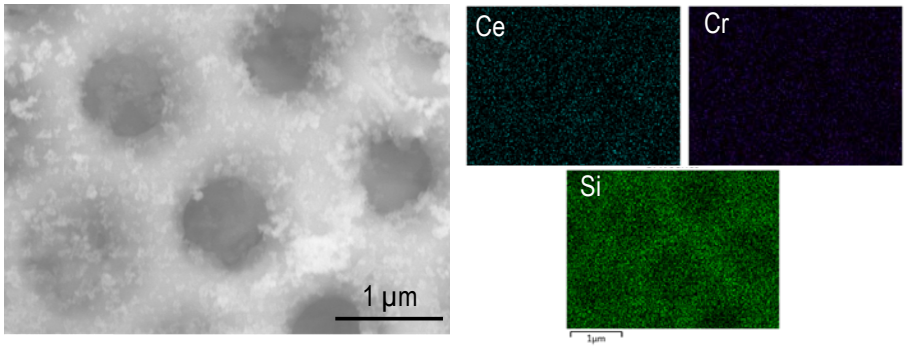

Figure 2-2. Scanning electron microscopy image of Cr-CeO_2 nanoparticles supported on kieselguhr, along with elemental mappings of the same area that were generated via energy dispersive X-ray spectroscopy. The Ce and Cr counts are due to the nanoparticles, and the Si counts are due to the kieselguhr supports.

To test for their water splitting capacity, the ceria-based nanomaterials were first reduced at 500 °C for an hour under flowing 2.9% H_2 in Ar (50 sccm). Then, the temperature was reduced to 400 °C, and water vapor in Ar carrier gas (50 sccm, saturated at 90 °C) was injected into the reaction chamber in 5.04 mL aliquot volumes (pulse chemie experiment). The gas composition downstream of the reactor was measured by a residual gas analyzer (RGA) to assess the water splitting capacity. These experimental runs were conducted using a Micomeritics AutoChem II 2920 automated catalyst characterization system. The RGA measurements for the different nanomaterials are shown in **Figure 2-3**. Neither the CeO_2 nor the Zr-CeO_2 nanoparticles generated any H_2 upon H_2O injection. On the other hand, both Cr-CeO_2 and Fe_2O_3-CeO_2 generated H_2 from each injection of H_2O, with the Fe_2O_3-CeO_2 nanoparticles generating approximately two orders of magnitude more than the Cr-CeO_2 nanoparticles.

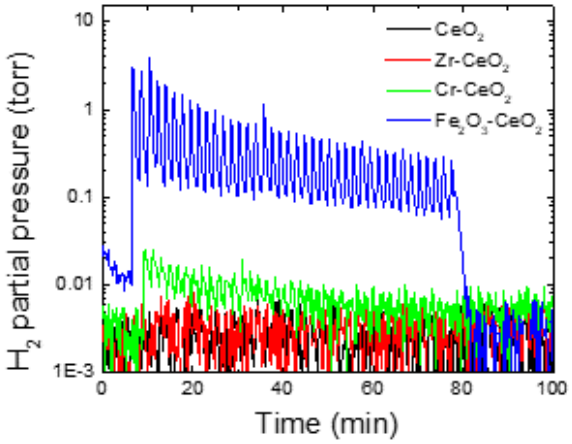

Figure 2-3. RGA measurements of water splitting using different ceria-based nanoparticles

Due to their superior performance, the Fe_2O_3-CeO_2 nanoparticles under went further testing to determine the effects of the substrate particles and to determine the long-term cycling performance. Two different substrates were compared, the Fe_2O_3-CeO_2 nanoparticles supported on kieselguhr and the Fe_2O_3-CeO_2 nanoparticles supported on alumina beads. **Figure 2-4a** shows a photograph of the different materials, while **Figures 2-4b – 2-4d** show their cycling behavior. After some initial variation, the Fe_2O_3-CeO_2 nanoparticles on alumina beads show a relatively stable cycling behavior, but they generate less hydrogen than the Fe_2O_3-CeO_2 nanoparticles supported on kieselguhr. The hydrogen generating capacity of the Fe_2O_3-CeO_2 nanoparticles supported on kieselguhr is initially much higher, but decreases with each cycle until cycle 5, where it stabilizes at a higher value than the nanoparticles supported on alumina.

The degradation of the water splitting capacity is attributed to nanoparticle agglomeration, as X-ray diffraction measurements revealed crystallite formation after the cycling tests. This is a challenge for nanoparticles in this application, as their structures can be inherently unstable and thermal cycling can provide the energy for structural changes. Further optimization of the nanoparticle dispersion and of the substrate particles could improve performance, but this may come at a detriment to the nanoparticle density, requiring much larger beds for implementation. It was decided at this point to investigate bulk materials with high surface areas that may be inherently more stable than nanoparticles during cycling.

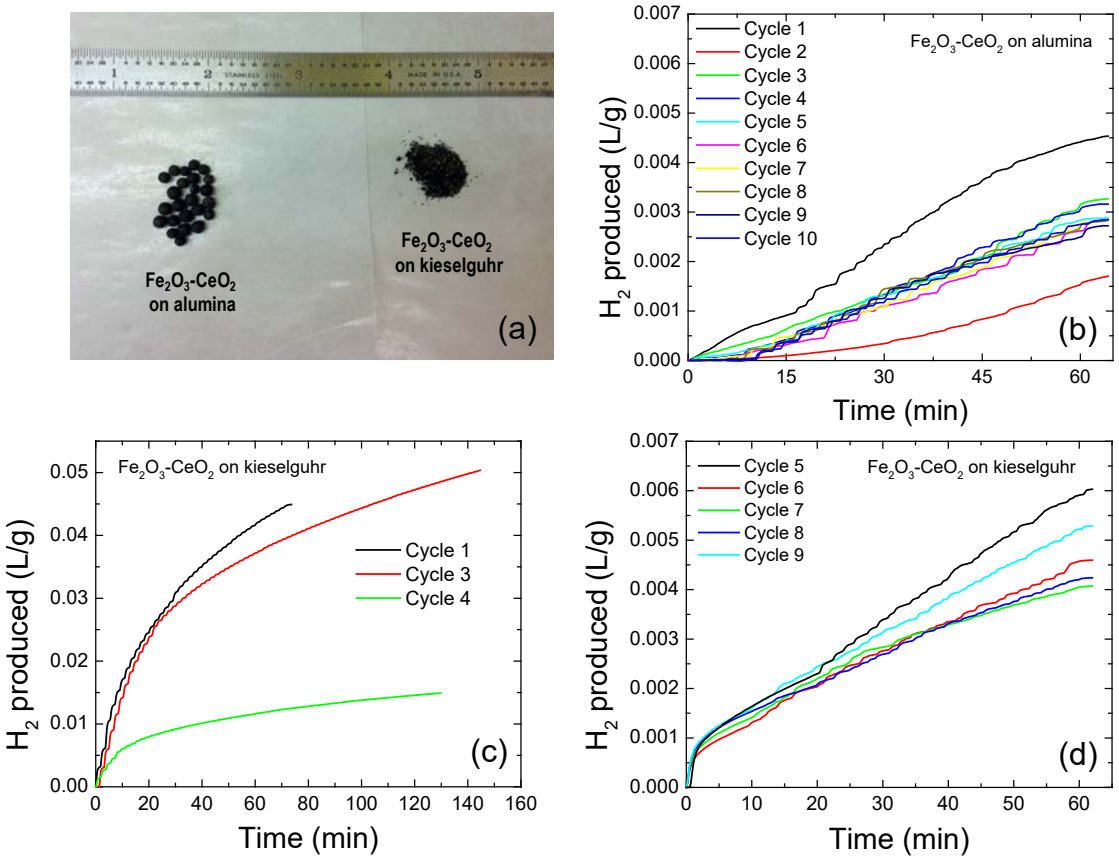

Figure 2-4. (a) Photograph of the Fe_2O_3-CeO_2 nanoparticles on different supports. RGA measurements from the cycling tests on (b) the alumina supports and (c) and (d) on the kieselguhr supports. Note, cycle 2 data is not included in (c) due to RGA malfunction.

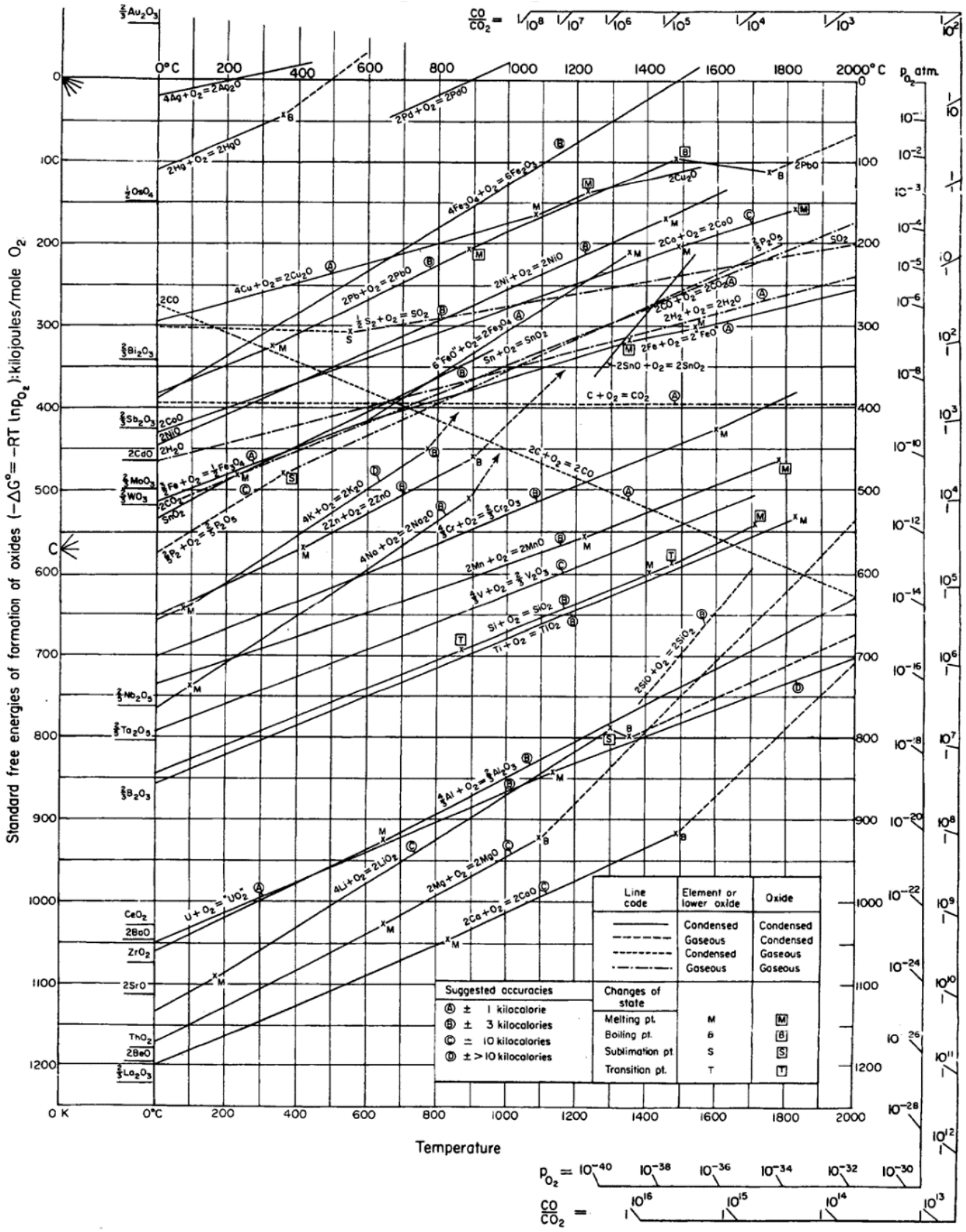

Figure 2-5. Ellingham Diagram

2.2 Porous Zero Valent Iron (p-ZVI)

In order to identify the optimal bulk material for reversible water splitting, one can consult thermodynamic data for metal oxides. The standard formation energies for oxides versus temperature and oxygen partial pressures are often presented in the form of Ellingham diagrams. A simple interpretation of these diagrams is that a metal can be oxidized (take oxygen from) a metal oxide that lies above it on the graph. By examining the Ellingham diagram shown in **Figure 2-5**, it is clear that the iron/iron oxide couple has optimal thermodynamic properties for cyclical water splitting as the formation energy intersects the formation energy line for hydrogen/water. That is, at higher temperatures hydrogen will strip oxygen from iron oxide, and at lower temperatures iron will strip oxygen from water. These optimal thermodynamic properties of iron/iron oxide are apparent in the nanoparticle study, as the Fe_2O_3-CeO_2 nanoparticles demonstrated the best water splitting properties.

In addition to optimal thermodynamics, iron/iron oxide has a number of other ideal properties for this process, including wide availability, chemical stability, and non-toxicity. Other metals with favorable thermodynamics do not exhibit these traits. For example, tin/tin oxide and carbon/carbon dioxide formation energies intersect the hydrogen/water line, as well, but these form a corrosive liquid metal (tin) and a gas (CO_2) upon reduction and oxidation, respectively. Thus, iron was selected as the bulk material of choice for reversible water splitting. In particular, porous zero valent iron (p-ZVI) was chosen due to its large surface area and low costs (**Figure 2-6**).

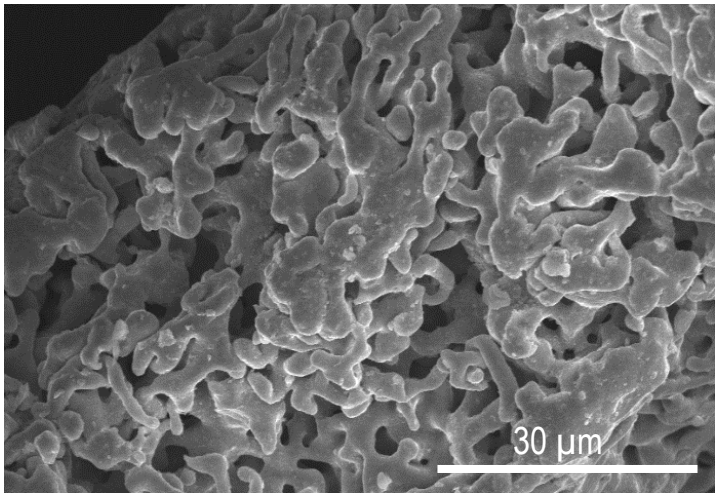

Figure 2-6. Scanning electron microscopy image of p-ZVI particle, highlighting the porosity and large surface area of the material.

Similar to the nanoparticle study, the water splitting capacity of p-ZVI was tested at different reduction temperatures 500 - 800 °C under flowing 2.9% H_2 in Ar (50 sccm), followed by water splitting at 500 °C, with saturated water vapor carried in Ar gas (50 sccm, saturated at 90 °C). As above, these experimental runs were conducted using a Micomeritics AutoChem II 2920 automated catalyst characterization system. The results are shown in **Figure 2-7a**. Except for the 600 °C reduction, the hydrogen produced during these runs are comparable to the volume produced by the Fe_2O_3-CeO_2 nanoparticles. **Figure 2-7b** shows the cyclical stability of the water splitting process, as p-ZVI can be cycled more than 10 times without any significant degradation of the water splitting capacity. While these results are encouraging, the amount of hydrogen generated per gram of p-ZVI needs to be increased. Otherwise, the beds will be far too large to fit into the glovebox space.

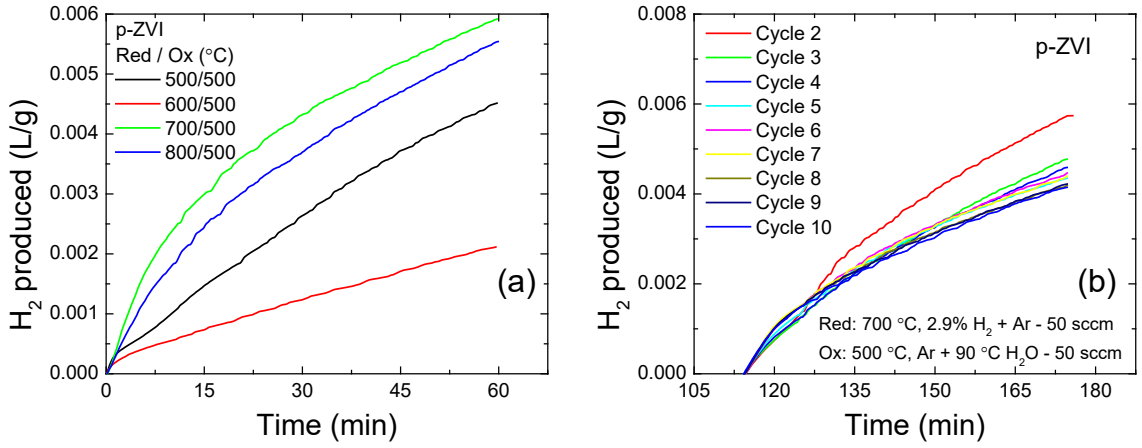

Figure 2-7. (a) Water splitting and (b) cyclical stability testing of p-ZVI

One way to improve the water splitting efficiency is by increasing the amount of iron oxide that is reduced to iron in the p-ZVI particles during the regeneration step. This can be done by increasing the concentration of H_2 gas during reduction from 2.9% to 100%, since this will have the same effect as reducing the relative oxygen partial pressure. Thus, cyclical water splitting experiments similar to the ones above were performed, except in this case the p-ZVI was reduced in 100% H_2 gas prior to water introduction. The results from these experimental runs are presented in **Figure 2-8**. As can be seen, the water splitting capacity for the p-ZVI increases by more than order of magnitude when pure H_2 gas is used for the reduction/regeneration step. Beds with increased water splitting capacities can easily be implemented within the glovebox space. For example, 4× 30 kg p-ZVI beds could process 150,000 STP-L of H_2O a year if each bed was regenerated about once per month, assuming an H_2 production capacity of 100 mL/g. 30 kg of p-ZVI occupies a volume of about 0.44 ft^3, which is a very reasonable size and could open additional glovebox space through the removal of larger mag beds. These results indicate that p-ZVI could serve as a regenerable replacement for magnesium metal in ZBR.

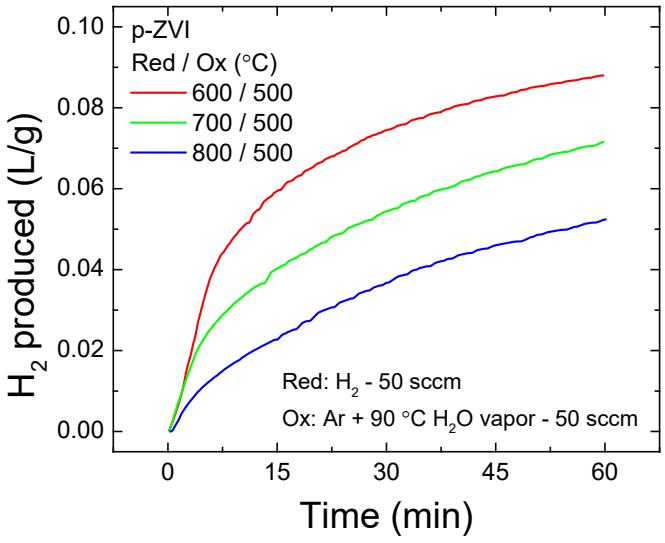

Figure 2-8. Water splitting testing of p-ZVI using 100% H_2 gas during the regeneration/reduction step

3.0 p-ZVI Process Parameter Testing

3.1 Overview

The positive results for p-ZVI materials described above indicate that p-ZVI beds could replace mag beds in the tritium facility in terms of water processing efficiency. However, there are a number of other factors that need further investigation before p-ZVI beds can be considered as a reasonable replacement for the mag bed process. For example, thermal and gas flow properties will determine how the p-ZVI bed will behave within a process environment, and the tritium decontamination factor will affect the disposal and processing route of the regeneration stream. This section addresses these and other considerations that will determine how a p-ZVI bed will perform in an industrial setting.

3.2 Morphology and Cyclic Stability

As seen above, the water splitting capacity of p-ZVI is stable over 10+ cycles for 2.9% H_2 reduction cycles. For the 100% H_2 reduction cycles, the water splitting capacity remained stable for over 20 cycles, after an initial decrease, from around 80 mL/g to around 60 mL/g, which could be attributed to morphological changes in the material. Therefore, scanning electron microscopy (SEM) imaging was conducted to observe any physical changes to the p-ZVI particles that may occur during cyclical water splitting. **Figure 3-1** shows micrographs of the surface of p-ZVI particles at increasing magnification, both before and after 20+ water splitting cycles. As can be seen in the images, the surface became smoother with smaller pores appearing after cycling. Image processing software (ImageJ) was used to measure the % area of the pores and statistical analysis of particle sizes in the SEM images before and after cycling. The pristine p-ZVI surface has an 18% surface porosity, while the cycled p-ZVI has a 9% surface porosity. The average pore size decreased from 2.7 µm to 0.4 µm after cycling. These assessments indicate that the pores are decreasing in size and density after repeated water splitting cycles. In addition to pore sizes, the overall particle morphology changes as well. There is a general decrease in average particle size after cycling. The results from this statistical analysis are shown in **Figure 3-2**. Notably, the longest and shortest sides of the irregularly shaped particles decrease by an average of 200 µm.

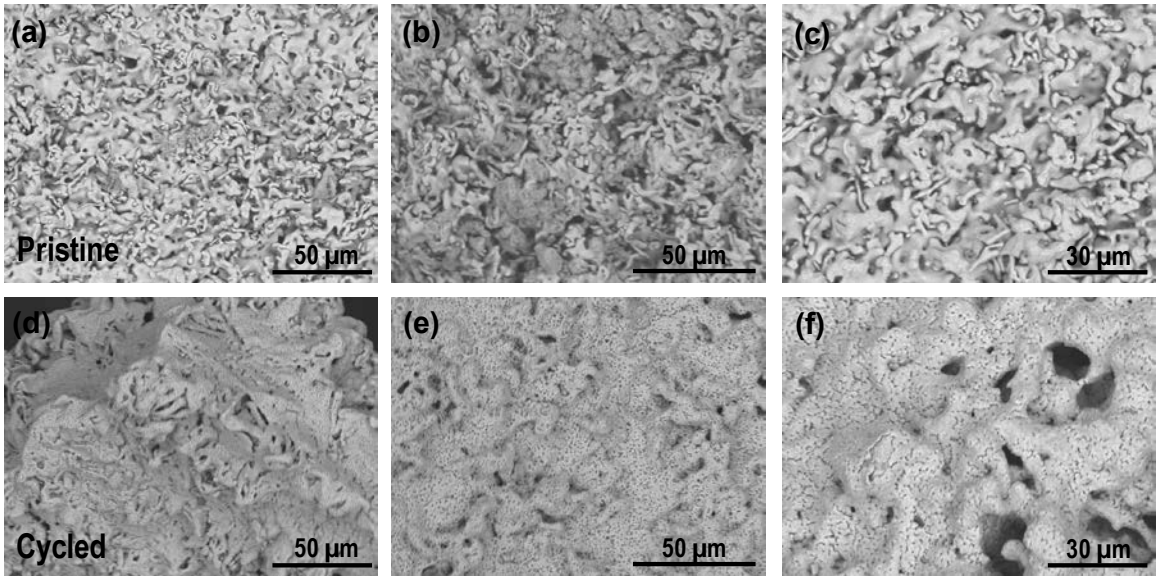

Figure 3-1. SEM images of the (a) – (c) pristine and (d) – (f) cycled p-ZVI particle surfaces at 1200×, 1500×, and 2000× magnifications, respectively.

Such particle decrepitation is not unexpected and is common for materials that are cycled at higher temperatures in hydrogen environments. Similarly, the sintering of the porous surface is also commonly observed in materials used for thermochemical water splitting. As described above, these morphological changes do not appear to significantly affect the long-term water splitting capacity of the p-ZVI. However, these morphological changes can impact the thermal and gas flow properties of the bed. Such effects will be considered in more detail below.

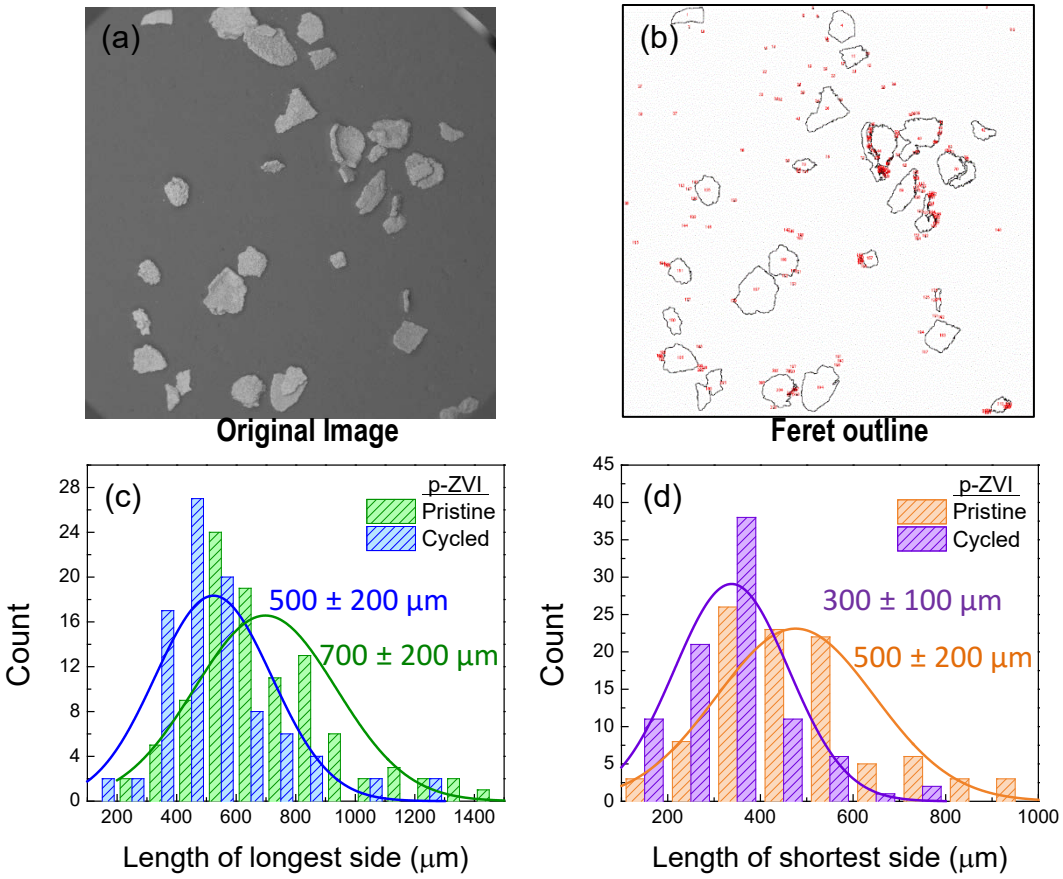

Figure 3-2. (a) SEM image and (b) ImageJ software extrapolation of the particles used for statistical analyses. Results of the image statistical analyses showing the particle counts and the lengths for the (c) longest and (d) shortest sides.

3.3 Thermal Properties

While isothermal cycles are possible, our results have shown that greater efficiencies are achieved when the regeneration and water splitting steps are done at different temperatures. Therefore, the thermal properties of p-ZVI are important parameters because these will help determine how fast these heating and cooling cycles can occur. In particular, the thermal conductivity, *k*, of p-ZVI will determine the rate of conductive heat transfer through the bed.

There are a number of different ways to measure the thermal conductivity of a substance, though powders and particulate materials present more of an experimental challenge. The technique employed here relies on the use of differential thermal analysis (DTA) [3-5]. The sample for which we want to determine the thermal conductivity is placed into a crucible in the DTA furnace, and a spherical calibration substance such as indium is placed on top of the sample (**Figure 3-3a**). The temperature of the calibration substance is fixed while it melts, creating a constant temperature

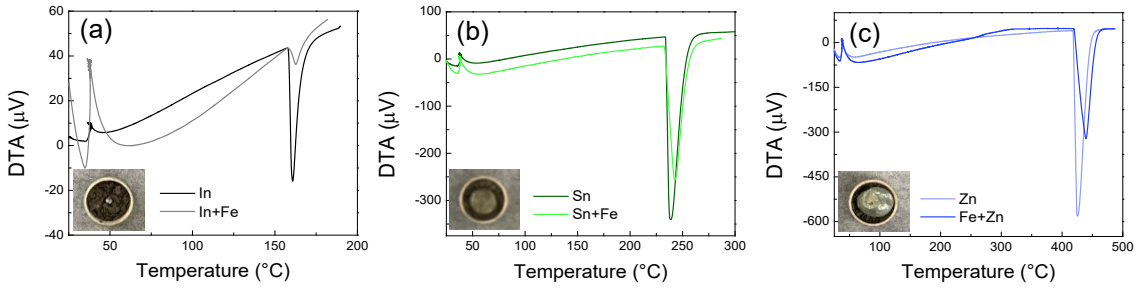

Figure 3-3. DTA measurement curves for the (a) – (c) In, Sn, and Zn calibration spheres, respectively, which were used for thermal conductivity extrapolation. Insets show the corresponding calibration spheres resting on the p-ZVI samples in the crucible.

boundary condition at the sample surface. A DTA scan is performed to measure the differential power produced during melting of the calibration substance, while it is resting on the sample. The resulting curve is approximately linear during the melting and decreases exponentially after melting is complete (**Figure 3-3**). The slope of the increasing part of the curve is proportional to the thermal conductivity of the sample, where the proportionality is also a function of the crucible and calibration sphere geometries. For the experiments performed here, we used DTA/TGA system and a sapphire calibration crystal to obtain the differential power curves. Indium, tin, and zinc spheres were used as calibration materials for the thermal conductivity measurements, and these have melting temperatures of T_m = 156.59, 231.95, and 419.59 °C, respectively. The advantage of this thermal conductivity measurement method is the ability to characterize small quantities of powders and particles using readily available analytical instruments.

The measured thermal conductivity of p-ZVI at the different calibration temperatures are presented in **Table 3-1**. The thermal conductivity of Al_2O_3 powder was also measured as a check on the experimental technique. The measured value is consistent with the literature values [4], which range from k = 0.1 – 0.3 W/m·K for Al_2O_3 powder. The measured thermal conductivity of the p-ZVI range from k = 0.071 W/m·K at 156.59 °C to k = 0.054 W/m·K at 419.59 °C. The result from the Sn measurement is presented in **Table 3-1**, but this k value is questionable as it appeared that Sn alloyed with the Fe surface and affected the experiment. It is important to note that the experiments were conducted in an Ar atmosphere and that the samples were pristine, uncycled p-ZVI. The thermal conductivity of a packed, porous bed will depend on background gas, so the k values will be higher in N_2 or H_2 atmospheres. Also, the thermal conductivity may change as the morphology and porosity of the p-ZVI particles change with cycling, as described in **Section 3.2**. The decrease in surface porosity will promote a higher thermal conductivity, while the decrease in particle size will tend to decrease thermal conductivity.

Table 3-1. Thermal Conductivity Measurements

Material	Temperature (°C)	Thermal Conductivity (W/m·K)
p-ZVI + In	156.59	0.071
p-ZVI + Sn	231.95	0.021
p-ZVI + Zn	419.59	0.054
Al_2O_3 + In	156.59	0.19

In order to get a better understanding of the p-ZVI dynamics, a simple COMSOL thermal model has been created. To simplify the geometry, a 2-dimensional axisymmetric model is used (Figure 3-4a), and the heat flow is simulated using a local, thermal, non-equilibrium, multiphysics model

that couples the heat transfer in solids and heat transfer in liquids calculations. The bed geometry is such that it can encompass 0.44 ft^2 of p-ZVI. p-ZVI particles are modeled as spherical pellets with an average pellet radius of $6.24x10^{-4}$ m, creating a packed bed with a porosity of 0.6. The solid is modeled as iron, the fluid as nitrogen, and the outer vessel as stainless steel. Outside, the bed is heated with a power of 500 W from an initial temperature of 773 K. The temperature versus time at the steel/p-ZVI boundary is plotted in **Figure 3-4b**, and a temperature map of the bed at 60 min is shown in **Figure 3-4c**. It takes about an hour for the bed to reach 873 K. Therefore, the bed temperature cycling does not appear to create an issue for fast regeneration of the p-ZVI beds. Finally, it's worthwhile to note that, due to its magnetic properties, p-ZVI could be heated via induction heating for faster thermal cycling.

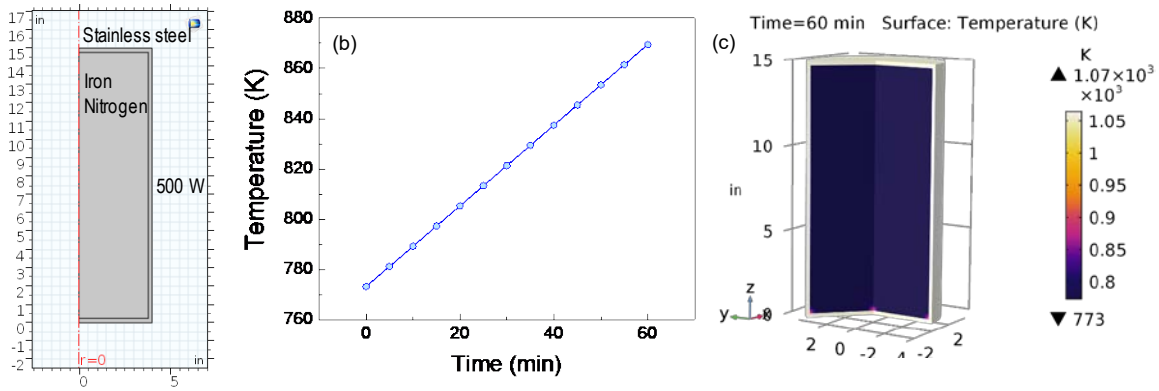

Figure 3-4. (a) Axisymmetric model of the p-ZVI bed. (b) Temperature versus time for a boundary probe located at the edge bed. The bed was initially 773 K and is heated on the outside using 500 W. (c) Temperature map of the modeled bed after 60 minutes of heating.

3.4 Gas Flow Properties

3.4.1 *Overview*

The Tritium Facility is a gas processing plant, and therefore, the way that product, reactant, and carrier gases interact with a p-ZVI bed will determine its behavior in an industrial setting. Important considerations include the pressure drop across the bed and the effects of carrier gases on the water splitting process. This section addresses these and other gas flow considerations for p-ZVI-based beds.

3.4.2 *Pressure Drop*

The pressure drop across a packed bed is an important parameter. Gas will not flow through a loop if the pressure drop is too large for the system's pump or blower. The pressure drop for a packed bed reactor can be calculated through the Ergun equation in the general case [6]. For laminar flows, the simpler Kozeny-Carman equation can be used:

$$\frac{\Delta P}{L} = -\frac{180\mu}{\theta^2 D_P^2}\frac{(1-\epsilon)^2}{\epsilon^2}u_s,$$

where ΔP = pressure drop; L = length of the bed, μ = fluid viscosity, θ = sphericity of the particles, ϵ = porosity of the bed, D_p = particle diameter, u_s = superficial velocity of gas. Thus, if the bed and particle geometries are known, the pressure drop for any system can be calculated.

To confirm that a packed p-ZVI bed obeyed the Kozeny-Carman equation, the pressure drop across packed p-ZVI beds (0.25" OD tubing, L = 0.13 m and L = 0.305 m) were measured using a differential pressure sensor at different gas velocities, u_s. The results are presented in **Figure 3-5**. The pressure drop as calculated by the Kozeny-Carman equation is also shown, where $\theta = 0.0119$ and $D_p = 0.698$ mm (both measured using ImageJ). The porosity value of $\epsilon = 0.5$ was selected as this gave the best fit for both bed lengths. Using these values, the pressure drop across a p-ZVI bed can be calculated for all laminar flows and bed sizes. In general, it can be expected that the pressure drop across a p-ZVI bed is less than 200 torr per meter for superficial gas velocities below 100 m/s.

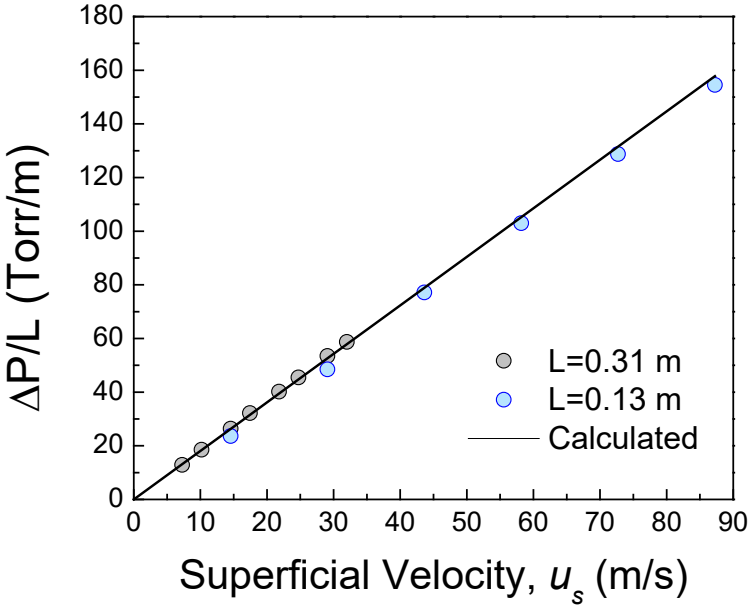

Figure 3-5. Measured and calculated pressure drop versus superficial velocity for p-ZVI beds with two different lengths.

3.4.3 *Carrier Gas*

Another concern for gas processing is the use of a carrier gas to move product and reactant gases through piping and loops in a system. In most of the experiments described above the carrier gas has been argon. While argon has a number of advantages experimentally, it is not an ideal choice for the Tritium Facility due to its higher cost and specific clean up requirements. The current practice for Z-bed recovery is to use a small amount of protium as a carrier gas during regeneration of the Z-beds. The balance between the amount of hydrogen and water is important for the p-ZVI water splitting process. If there is too much hydrogen relative to the water, then the reaction will be driven toward the greater reduction of iron oxide to iron via hydrogen, instead of the oxidation of iron to iron oxide via water.

The effects of hydrogen as a carrier gas on p-ZVI were investigated by performing water splitting experiments, where the carrier gas for the water vapor was either 100% H_2 or 2.9% H_2 in Ar. For the 100% H_2 carrier gas, no water splitting was observed over the p-ZVI, as the atmosphere was too reducing for water splitting to occur. However, for the 2.9% H_2 in Ar carrier gas, water splitting was observed (**Figure 3-6**). The ratio of H_2 to H_2O partial pressures is approximately equal to one in this case. Therefore, H_2 may still be used as carrier gas for the p-ZVI process so long as the

partial pressure of H_2 does not exceed that of H_2O. While not investigated here, N_2 could also be potentially used as a carrier gas. Iron nitrides do not form in N_2 gas at the temperatures investigated here, and the Sieverts equation predicts a nitrogen uptake of only 0.0009 weight % in iron at 500 °C [7, 8].

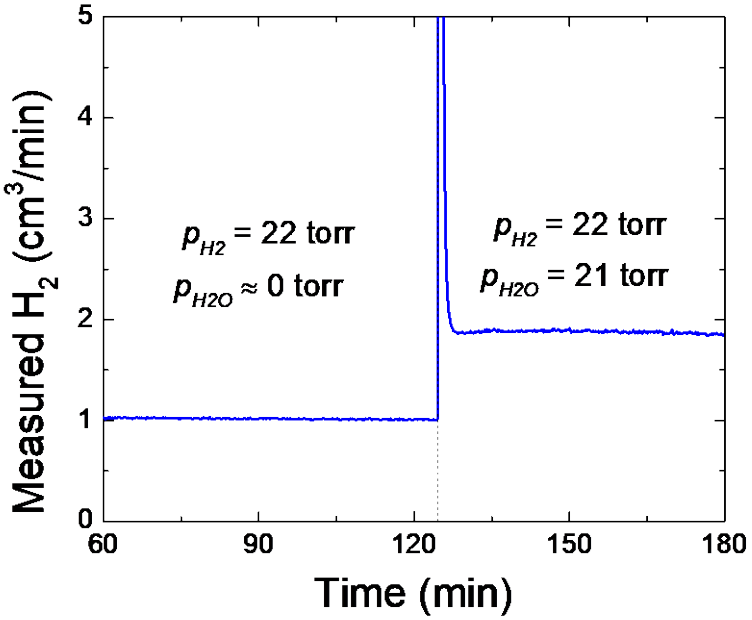

Figure 3-6. Measured H_2 during p-ZVI water splitting experiment when 2.9% H_2 in Ar was used as the carrier gas for water vapor. The dotted line indicates when the water vapor was introduced. The listed partial pressures describe the product gases that are introduced into the reactor.

In a circulating system, the balance between H_2 and H_2O will change as p-ZVI cracks water to form hydrogen. Therefore, the excess hydrogen product could be removed from the loop via a palladium membrane, for example, to keep the hydrogen partial pressure below that of water. Alternatively, the circulating system could be run until the hydrogen and water partial pressures are equal, then the loop could be evacuated through the cooled and dried Z-bed, capturing the remaining water and sending the hydrogen product on to further processing. In the latter case, the useable loading capacity of the Z-bed is reduced by half. This feature would have to be weighed against the positive benefit of having regenerable p-ZVI beds instead of single use mag beds. Finally, another possibility is to take advantage of increased hydrogen to water ratios for partially consumed p-ZVI. As shown, in **Figure 3-7**, the H_2/H_2O ratio during water splitting on p-ZVI is a function of bed oxidation. Therefore, it is possible to dry the H_2 product gas more completely without the use of a palladium membrane by reducing the amount hydrogen produced per gram of p-ZVI. Conceptually, this is similar to using a palladium membrane in the reactor, but in this case the product that is being removed is the iron oxide, instead of the hydrogen. This route will require larger beds and/or fast regeneration cycles, but will allow for process optimization over the one-to-one ratio for hydrogen to water.

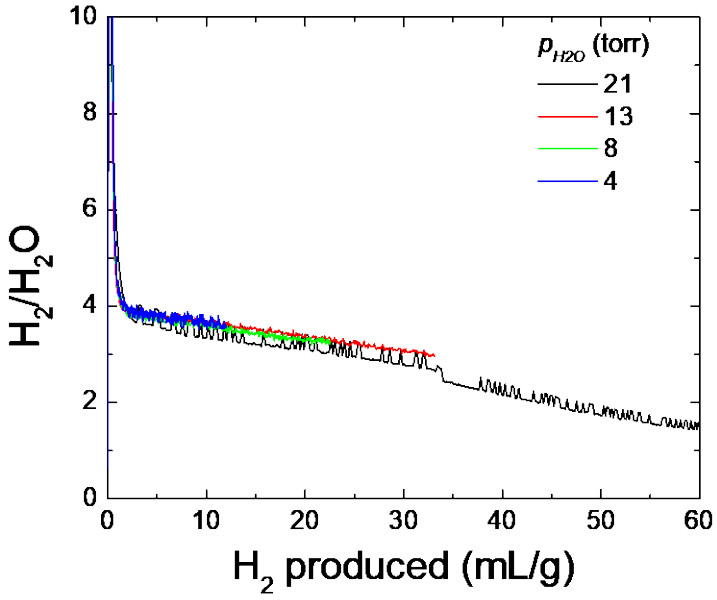

Figure 3-7. Measured H_2/H_2O ratio during p-ZVI water splitting experiments where different water partial pressures were introduced into the reactor. The H_2/H_2O ratio decreases as more H_2 is produced and the p-ZVI is converted to iron oxide.

3.5 Tritium Decontamination Factor

Most of the previous discussion has focused on the water splitting properties of p-ZVI, but an equally important component of the p-ZVI process is the regeneration cycle. In this case, the clean water produced during the hydrogen reduction of p-ZVI must be sufficiently clean for disposal. That is, little to no cross-contamination from the cracked tritiated water into the water produced during regeneration cycle should be detected.

Experiments were performed to measure this cross-contamination using the Micomeritics AutoChem II 2920 automated catalyst characterization system and using deuterium as a surrogate for tritium. In these experiments, a D_2O-H_2O mixture (8200 ppm D_2O) was passed over a reduced p-ZVI sample for 60 minutes at 500 °C. Then, the sample was heated to 600 °C and regenerated for the same amount of time in hydrogen gas. During the regeneration cycle, the product gases were routed through a cold trap to collect the water produced by the reduction of p-ZVI. This cold trap was bypassed during the water splitting experiments. The water collected during regeneration was analyzed using cavity ring down spectroscopy to measure the concentrations of hydrogen isotopes. For these experiments, a decontamination factor (DF) was calculated, where the DF is equal to the ratio of the concentration of D_2O in the water splitting cycle to the concentration of D_2O recovered in the cold trap during the regeneration cycle. The DF for the p-ZVI water splitting process was found to be DF > 134.

It is worth noting that this initial DF value is already much greater than those reported for commercial catalytic exchange columns (DF = 25 - 35) currently used for detritiation and approaches detritiation targets for cooling water at TVA Watts Bar (DF = 140) [9]. With further optimization, the single stage DF could be improved to higher values, and final implementation within the Tritium Facility will depend on emissions targets, as will be discussed below. Cost-benefit analyses against other detritiation processes are needed for commercial applications, but the advantages of implementing regenerable p-ZVI beds in a detritiation process over using other techniques include low cost materials (Fe vs. Pt), hydrogen recycling, simplicity (no electrolyte or

permeable membrane), safety (no oxygen stream), and lower energy (vs. combined electrolysis catalytic exchange).

4.0 Implementation of the p-ZVI Process

4.1 Overview

The stripper systems in the Tritium Facility remove tritium by combustion with ambient oxygen to form water, which is subsequently collected on Z-beds, along with a large quantity of water that makes its way into the gloveboxes from the process rooms. To process the hydrogen isotopes from this water, the oxygen must be separated from the hydrogen, safely secured, and removed from the facility. There are three disposal routes for this oxygen - it can leave as a solid, liquid/vapor, or a gas. The current process relies on trapping oxygen in a solid form (magnesium oxide). Disposal routes using liquid and gas phases will be discussed below.

4.2 H_2 Regeneration

This report has focused on the development of the p-ZVI process where the regeneration process uses hydrogen gas to reduce the iron oxide back to iron, creating a liquid/vapor stream of "clean" water for disposal. The advantages of this process are that no new process gases are required, only moderate temperatures are used, and disposal could be easier than solid pathways, depending on the DF of the process. Another advantage is that the concept is very similar to the current process, except that a non-regenerable mag bed is replaced by regenerable p-ZVI beds. If a palladium membrane is incorporated into the reactor design, such as in Ref. [10], then there should be minimal impact on the downstream hydrogen isotope processing. The primary changes then, will be in the incorporation of the regeneration process. The incorporation of a hydrogen source for regeneration will be straightforward. The output path for the regeneration stream requires further consideration.

The disposal path for the regeneration stream needs to be determined, and there are a few options. Direct disposal down the drain seems unlikely, as the cleanup requirements for this exceeds the capacity for any known process that can fit within the existing glovebox space. One alternative is to dispose of the regeneration water by trapping it within a solid (cement, AMSBs) for disposal as solid waste. Determining whether such a process will reduce the costs and efforts when compared to mag bed disposal requires further study. A more easily implemented solution is simply to stack the regeneration water, releasing any associated residual tritium as tritium oxide emissions. The primary concern with directly stacking the regeneration stream is minimizing the tritium process loss and minimizing tritium releases to the environment. In order to get a better understanding and to quantify the issue, **Table 4-1** lists the quantity in grams of T_2O versus parts-per-million (ppm) for 150,000 STP-L of water vapor, which was approximately the total water processed by Z-bed recovery per year according to 2013 data but may be lower now [1]. From a facility perspective, the acceptable T_2O release quantities in grams corresponds to a target ppm released from the p-ZVI process.

Table 4-1. T_2O grams versus parts-per-million (ppm) for 150,000 STP-L of water vapor

ppm	T_2O (g)
1	0.12054
5	0.60268
10	1.20536
20	2.41071
30	3.61607
60	7.23214
100	12.05357

Thus far, the p-ZVI process has demonstrated a DF > 134, which corresponded to a reduction in D_2O from around 8200 ppm to 60 ppm. Assuming that 8200 ppm is a typical T_2O concentration in Z-bed recovery, then 60 ppm would result in an unacceptable loss of tritium according to **Table 4-1.** Decontamination to <5 ppm would be more acceptable. It is important to note that the measured p-ZVI DF value reported here is based on initial exploratory experiments and there is further room for optimization. First, the size of p-ZVI sample was much smaller than the wetted components of experimental system during DF testing, so it is highly likely that most of the residual D_2O seen in the regeneration stream came from other components and piping and not from the p-ZVI, especially from regions that were at much lower temperatures than the reactor section. The DF factor will be higher in larger scale systems, where the reactor size is much larger than the shared manifolds. Prototype systems that do not use shared piping will also see higher DFs. Also, the water splitting and regeneration cycles were run back to back in the experiment described in **Section 3.5**. Evacuating the reactor or providing some isotopic swamping in between cycles will further increase the DF. The main goal for further research into the p-ZVI process should be to optimize the reactor and process to further minimize the cross-contamination between cycles.

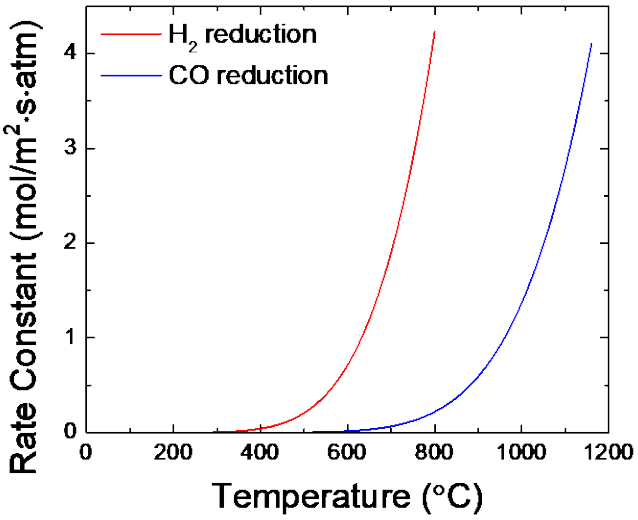

Figure 4-1. Calculated reaction rate constants for the reduction of iron oxide by carbon monoxide and hydrogen gas

4.3 CO Regeneration

The primary focus of the research so far has been the use of hydrogen gas as a reducing agent to regenerate the p-ZVI bed for cyclical water splitting. It is also possible to regenerate p-ZVI using carbon monoxide: Fe_xO_y (solid) + CO (gas) → Fe (solid) + CO_2 (gas, waste). The introduction of a carbon monoxide/dioxide stream within the Tritium Facility will present some challenges, mostly due to the potential for the introduction of carbon species into other gas streams. Therefore, the cross-contamination from the regeneration stream (CO/CO_2) to the water splitting stream will need to be characterized, in addition to the tritium pickup by the regeneration stream. On the positive side, since there would be no isotopic exchange between any retained tritium and the regeneration gas, it is expected that the DF for CO regeneration would be greater than the DF for H_2 regeneration. A final consideration for CO regeneration is kinetics and thermodynamics. The reduction of iron oxide by carbon monoxide is slower and requires more energy than the reduction of iron oxide by hydrogen. Using parameters found in the literature [11], the rate constants for the reduction of iron oxide by hydrogen gas and by carbon monoxide have been calculated. The results are presented in **Figure 4-1**, and it can be seen that reaction rate constants for CO reduction are much smaller than

the rate constants H_2 reduction for all temperatures. According to the calculations, a temperature of 920 °C is necessary for CO reduction to match the same rate constant for H_2 reduction at 600 °C. These higher temperatures could impact particle stability and lead to increased tritium permeation. Additionally, incorporation of palladium alloys with a CO process is difficult. Thus, while the CO reduction process may be technically feasible, the use of H_2 for regeneration of p-ZVI has more advantages. However, if the of H_2/H_2O regeneration stream process becomes infeasible due to disposal concerns, the CO/CO_2 regeneration cycle could be investigated.

5.0 Conclusions

The research presented above describes investigations into the reduction-oxidation cycles of metal/metal oxides for the purpose of creating a reusable water splitting system to replace the mag beds in the Tritium Facility. After an experimental down-selection, porous zero valent iron (p-ZVI) was identified as an ideal candidate metal due to its low cost, large hydrogen generation capacity, and moderate operational temperatures. Additional investigations of p-ZVI were conducted to better understand how a bed composed of such material would behave in the facility. The long-term cycling behavior of p-ZVI was found to be stable. The thermal conductivity of the material was adequate, and the pressure drops across p-ZVI beds were found to be easily manageable. An initial decontamination factor was found for the p-ZVI process, which exceeded commercial processes. While higher decontamination factors may be desirable, the process has plenty of room for optimization of the decontamination. These results indicate that p-ZVI beds could serve as low cost, reusable replacements for mag beds in the Tritium Facility. Future research should be devoted to building a larger scale, prototype system so higher decontamination factors can be established. In addition, the incorporation of a palladium alloy membrane into the reactor should be investigated, as this will simplify the delivery of clean and dry hydrogen isotopes to downstream systems.

6.0 References

1. Klein, J.E., K.L. Shanahan, and J. Wilson, *Tritium Facilities Magnesium Bed Reduction/Elimination Study.* SRNL-TR-2013-00198, Rev. 0, 2013.

2. Singh, P. and M. Hegde, *Ce0. 67Cr0. 33O2. 11: A new low-temperature O2 evolution material and H2 generation catalyst by thermochemical splitting of water.* Chemistry of Materials, 2009. **22**(3): p. 762-768.

3. Camirand, C.P., *Measurement of thermal conductivity by differential scanning calorimetry.* Thermochimica Acta, 2004. **417**(1): p. 1-4.

4. Pujula, M., et al., *Measuring thermal conductivity of powders with differential scanning calorimetry.* Journal of Thermal Analysis and Calorimetry, 2016. **125**(2): p. 571-577.

5. Sánchez-Rodríguez, D., et al., *Determination of thermal conductivity of powders in different atmospheres by differential scanning calorimetry.* Journal of Thermal Analysis and Calorimetry, 2015. **121**(1): p. 469-473.

6. Ergun, S. and A.A. Orning, *Fluid flow through randomly packed columns and fluidized beds.* Industrial & Engineering Chemistry, 1949. **41**(6): p. 1179-1184.

7. Epstein, S. and J. Wymore, *Observations on the iron-nitrogen system.* Stahl und Eisen, 1923. **43**: p. 1271.

8. Ertl, G., M. Huber, and N. Thiele, *Formation and decomposition of nitrides on iron surfaces.* Zeitschrift für Naturforschung A, 1979. **34**(1): p. 30-39.

9. Brooks, K., G. Sevigny, and E. Love. *Review and Evaluation of Water Detritiation Technologies for Watts Bar Primary Cooling Water*. in *Tritium Focus Group Meeting*. 2017. Pacific Northwest National Laboratory.

10. Modica, G. and R.A.H. Edwards, *A Reactor-Permeator for Reduction of Tritium Oxide on Iron.* Fusion Technology, 1995. **27**(2T): p. 75-78.

11. Hayes, P., *The kinetics of formation of H2O and CO2 during iron oxide reduction.* Metallurgical Transactions B, 1979. **10**(2): p. 211-217.

Distribution:

S. L. Marra, 773-A
T. B. Brown, 773-A
D. R. Click, 999-W
S. D. Fink, 773-A
C. C. Herman, 773-A
E. N. Hoffman, 999-W
F. M. Pennebaker, 773-42A
W. R. Wilmarth, 773-A
Records Administration (EDWS)

R. W. Allgood, 999-2W
D. W. Babineau, 773-A
J. L. Clark, 246-1H
H. Mentzer, 246-1H
D. Cyr. 246-1H

G. K. Larsen, 999-2W
S. E. H. Murph, 999-2W
L. M. Angelette, 999-2W
K. J. Lawrence, 999-2W